International Journal of Agriculture and Environmental Research

ISSN: 2455-6939

Volume: 08, Issue: 01 "January-February 2022"

SEASONAL AND DIURNAL VARIATION OF SURFACE ENERGY FLUXES AND SURFACE CHARACTERISTICS OVER A SEMIARID GRASSLAND IN WEST AFRICA

[1*]Oluwadare Ayoola O., [2]Kunstmann Harald, [3]Oluwadare Esolomo J., [4]Bliefernicht Jan

[1]Elizade University, Ilara Mokin, Ondo State, Nigeria.

[2]Institute of Meteorology and Climate Research, Karlsruhe Institute of Technology (KIT), Germany.

[3]Ajayi Crowther University, Oyo, Oyo State, Nigeria.

[4]Regional Climate and Hydrology, University of Augsburg, Germany.

*Corresponding Author

DOI: https://doi.org/10.51193/IJAER.2022.8107

Received: 18 Jan. 2022 / Accepted: 26 Jan. 2022 / Published: 02 Feb. 2022

ABSTRACT

Radiative fluxes and surface energy fluxes computed using the eddy covariance method from January to December 2013 were used to investigate the partition of energy and energy exchange over degraded grassland in the Sudanian savannah region of West Africa. In Sumbrungu Agunsi, (10.841°N, 0.918°W), in Ghana's upper east area, an Eddy Covariance station was erected near to the Ghana–Burkina-Faso border. The fluctuations in radiation components, energy fluxes, and surface characteristics components were studied on a seasonal and daily basis. The Incoming shortwave radiation, out-going shortwave radiation, incoming long wave radiation and out-going long wave radiation all varied annually, resulting in a seasonal variation in net radiation. The soil moisture content, evaporative fraction, and the surface albedo were found to be low during the dry season but high during the wet season, while, the Bowen ratio was found to be high during the dry season but low during the wet season. During the wet season, majority of the available energy were converted to latent heat, but, during the dry season, majority of the available energy was transformed to sensible heat. The station's energy balance closure was investigated; slope of the regression found was 0.67 with an intercept of 33 Wm^{-2}. The reasons for the station's energy balance not being closed were investigated.

Keywords: Radiative fluxes, Energy Fluxes, Surface characteristics, Eddy Covariance.

ISSN: 2455-6939

Volume: 08, Issue: 01 "January-February 2022"

1. INTRODUCTION

Over the last few decades, the land surface of West Africa has changed dramatically as a result of different anthropogenic activities. The effects of these land surface changes in conjunction with climate change on meteorological fluxes are unknown, preventing the development of useful adaptation mechanisms for long term management of water, agriculture and other natural resources like renewable energy. Heat, water vapour and carbon dioxide exchange between the ground surface and atmosphere have recently gotten attention since they not only play a big part in local convection, but they also have a big impact on local climate especially during monsoon onset and withdrawal of monsoon. (Xue et al., 2004, Toda et al., 2002,). The surface fluxes of heat, moisture and momentum determine the steady state of the atmosphere to a great extent (Beljaars and Holtslag, 1991).

In agro-meteorology, hydrology, climatology and atmospheric sciences, the equilibrium in the radiative energy fluxes at the earth's surface has been discovered to be of great interest. Climate simulations also react to small changes in surface partitioning of this radiative energy into sensible and latent heat fluxes either during seasonal or diurnal variations (Dickinson et al., 1991). Charney (1975) discovered that an increase in the surface albedo causes a loss of the absorbed radiative energy at the surface and reduces convective overturn in the semi-arid environments.

As a result, the likelihood of precipitation is reduced. Several studies have since demonstrated the importance of surface-to-atmosphere exchanges over West Africa as a result of Charney's result. It was discovered that the interactions of the land surface-to-atmosphere transfer over West Africa influence the frequency of rain in the arid region (Taylor et al., 2012, Fuller and Ottke 2002, Taylor and Lebel, 1998, Nicholson et al., 1998).

In the last 50 years (1970 to 2020), the population in West Africa has expanded by a factor of four and is predicted to quadruple by 2050 according to the UN's most optimistic prediction (UN, 2019). As a result, this population growth, natural vegetation areas are being converted to cultivated area on a constant basis. As the population of the Semi-arid regions (West Africa) grows, natural vegetation areas damaged as a result of intense human activities, especially since farming and cattle keeping are the primary occupations of people who live there (Dixon *et al*., 2001). The variations in energy exchange between the surface and atmosphere could be influence by this change in land cover and land use (Mamadou *et al*., 2014). As a result, research based on in-situ data are required to improve knowledge of the processes driving energy partitioning at the surface in this region, as well as to assess the consequences of land cover changes on the surface-to-atmosphere energy exchanges.

ISSN: 2455-6939

Volume: 08, Issue: 01 "January-February 2022"

In August 1992, during the transition from rainy to dry season, one of the first Eddy Covariance EC studies was conducted in West Africa at a field located in the Sudanian Savannah of Southern Niger (Verhoef *et al*., 1996). Another attempt was made over a fallow bush at a site in Nigeria during the transition period between February and March, where heat fluxes for three different weather scenarios were analysed (Jegede *et al*., 2004). Mauder *et al*., (2007) focused on the site's energy balance closure. Furthermore, EC stations have been installed at numerous location throughout West Africa, providing flux measurements over time in varied land cover types (Oluwadare et al., 2018, Mamadou *et al*., 2014, Wilson et al., 2002, Timouk *et al*., 2009). Due to changes in water regime and vegetation type, they observed spatial variability of surface fluxes across different land types. This study analyse a year's worth of Eddy Covariance flux measurements obtained in Sumbrungu Agunsi, Ghana's Upper East region, from a heavily degraded site with extensive agricultural activities. The goal of this study is to look at the seasonal and daily fluctuations in solar radiation components, energy fluxes, surface characteristics and the energy partitioning in a Semi-arid region in Ghana.

2. MATERIALS AND METHODS

2.1 Description of the Study Area

In Vea catchment, some 35 km drive away from Bolgatanga (a large city) in Ghana's Upper East region, an Eddy Covariance (EC) station was erected in a community called Sumbrugu Agunsi (10.841°N, 0.918°W), with elevation of 190 m above sea level (ASL) . Figure 1 depicts a location map of the research area. The figure also depicts the distance between the study region and the nearest large city. The terrain is quite flat, and is heavily deteriorated due to extensive agricultural activities. The region around the EC station is largely used as grazing land for various cattle (which include, cow, sheep, goat). Short grasses (*Brachiaria lata, Chloris piloasa and Cassia mimosoides*, with an average height of 0.10 m when fully grown) coexist with dispersed trees (dominated by *arkia biglobosa, Adansonia* and *Lannea microcarpa*) with heights ranging from 5 to 7 m and spacing of 30 to 40 m. However, the vegetation around the EC station is primarily grasses with a height of 0.10 m when fully grown in the rainy season.

2.2 Climate of the Study Area

The climate and vegetation of the site are typical of the Sudanian savannah, with a monomodal rainy season that lasts from May to October and a dry season that starts in November and last until April (Callo-Concha *et al*., 2012). Dry and dusty harmattan winds dominate the dry season, with cool night air temperatures and low relative humidity. The Inter-Tropical Discontinuity (*ITD*), influences the climate of this region. Temperature in the region ranged from 22 to 40

ISSN: 2455-6939

Volume: 08, Issue: 01 "January-February 2022"

degree Celsius, with an annual relative humidity ranging between 6 to 95 percent and annual rainfall ranging from320 and 1100 millimeters.

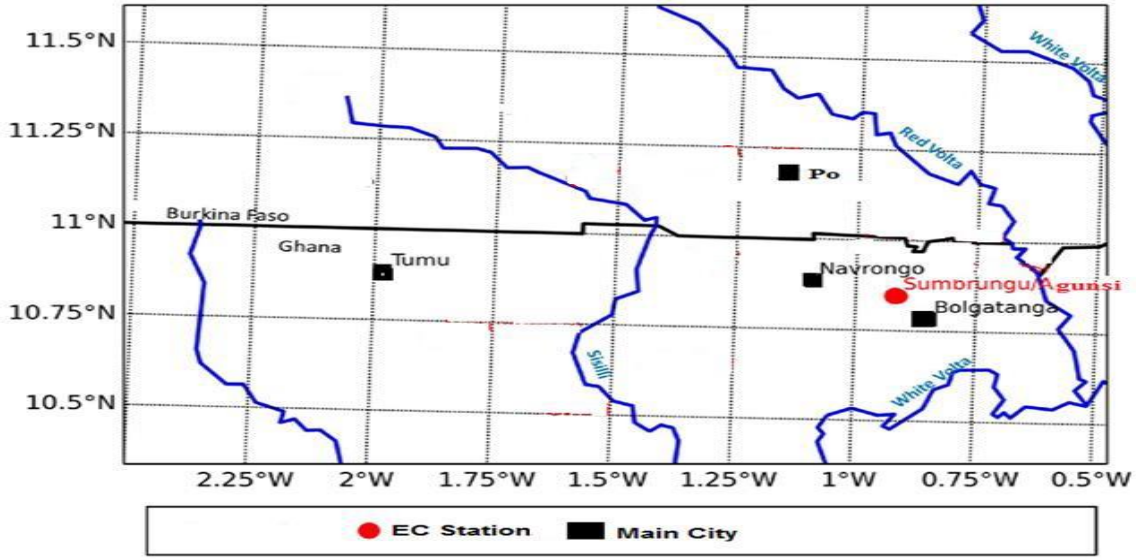

Figure 1: Location map of the study area

2.3 EC Station Instrumentation

In order to monitor the net radiation, sensible, latent, and ground heat fluxes in the site, an EC station was installed. This station had a three-dimensional sonic anemometer (CSAT3 Campbell Scientific, USA) that measured the three-dimensional wind vector, virtual temperature, and wind direction, as well as an open-path CO_2 and H_2O infrared gas analyser (LI-7500A, LI-COR Biosciences, USA) that measured turbulence fluxes of carbon fluxes and water vapour density. These data were taken at a rate of 20Hz and averaged over 30 minutes. The sensors were installed on a 4 m tall mask. A Net radiometer (CNR4, Kipp & Zonen, Netherlands) was also installed to measure incoming and outgoing shortwave and longwave radiations, as well as an HMP155A (Campbell Scientific, USA) to monitor temperature and relative humidity. The experiment set up in the station is shown in Figure 2.

ISSN: 2455-6939

Volume: 08, Issue: 01 "January-February 2022"

Figure 2: Installation set up at the EC station.

A Pluviometer and a tipping bucket were used to measure rainfall. Air temperature, Precipitation, relative humidity, air pressure, horizontal wind speed and direction were all measured using a multi-sensor WXT 520 (Vaisala, Finland). To detect soil moisture content, CS616 soil moisture content probes (Campbell Scientific, USA) were implanted. To monitor soil temperatures and heat fluxes, three sets of TCAV temperature probes with four sensors (Campbell Scientific, USA) and three HFP01SC heat flux plates (Hukseflux, Netherlands) were implanted below the ground surface. Three soil heat flux sensors were placed at a depth of 8 cm from the surface with a 5 cm separation, and three sets of soil temperature sensors, each containing four sensors, were used to measure soil temperature from the surface to depths of 3 cm, 10 cm, and 30 cm, respectively, with each set of soil sensors being averaged. At a depth of 3 cm, three soil moisture probes were placed. The energy storage in the layer of soil between the surface and the heat flux plate at a depth of 3 cm was calculated using soil temperature and moisture probes.

Mauder and Foken (2011) developed an EC software program TK3.1 which was used to process the EC data. From a 30-minute covariance between vertical wind velocity and air humidity or temperature, the latent and sensible heat fluxes were calculated. The following settings were utilized in the TK3 software: After Vickers and Mahrt (1997) proposed spike detection (i.e. values exceeding 4.5 times the standard deviation of the last 15 values were labeled as spike), the planar fit approach for coordinate rotation with time periods between 7 and 12 days was

ISSN: 2455-6939

Volume: 08, Issue: 01 "January-February 2022"

proposed (Wilczak et al., 2001). The approach described by Schotanus et al., (1983) was used to convert acoustic temperature to real temperature, and density fluctuation correction was performed using the adjustment proposed by Webb et al., 1980. The scheme following (Foken et al., 2004) was utilized for data quality analysis. Only half-hourly values for friction velocity, sensible heat flux, and latent heat flux with flags 0 and 1 (indicating high-quality data acceptable for fundamental study) were evaluated.

The energy balance was driven to closure using the Bowen ratio (Twine et al., 2000) to adjust for the non-closure, and the corrected fluxes were estimated using;

$$LE_{cor} = \frac{R_n - G}{\beta + 1} \quad \text{.......(1)}$$

$$H_{cor} = R_n - G - LE_{cor} \quad \text{.......(2)}$$

Where R_n is the net radiation, G is the ground heat flux, H is the sensible heat flux, LE is the latent heat flux, LE_{cor} is the corrected latent heat flux, H_{cor} is the corrected sensible heat flux and β is the bowen ratio (H/LE), where H and LE are the values estimated by the EC system.

While, the ground heat flux G was calculated by combining the measured ground heat flux G_m with the rate of change of heat storage G_s above the heat flux plate which was at 3 cm depth.

$$G = G_m + G_s \quad \text{.......(3)}$$

Where, G_s was computed based on the equation proposed by Liebethal*et al.*, 2005.

$$G_s = \int_0^z c_v \frac{\partial T}{\partial t} dz \quad \text{.......(4)}$$

Where c_v is the volumetric heat capacity, z [m] is the depth above the heat flux plate, T [°C] is the soil temperature measurements at 3 cm, and t[s] is the time intervals. c_v was computed from the composition of the soil following the equation given by De Vries (1963);

The evaporative fraction EF defined as the ratio of the latent heat to the available energy at the land surface, is assumed to be constant during the day time hour (Brutsaert and Sugita, 1992, Farah *et al.*, 2004). EF was estimated from the eddy covariance data using:

$$EF = \frac{LE}{LE + H} \quad \text{.......(5)}$$

ISSN: 2455-6939

Volume: 08, Issue: 01 "January-February 2022"

3. RESULT AND DISCUSSION

3.1 Meteorological Conditions over the Study Areas

At the EC site, the meteorological conditions (air temperature and relative humidity) over the study area were assessed. In the year 2013, the daily averages of wind speed, daily precipitation, air temperature, absolute humidity, soil water content SWC, and vapour pressure deficit for the site are shown in Figures 3a-b.

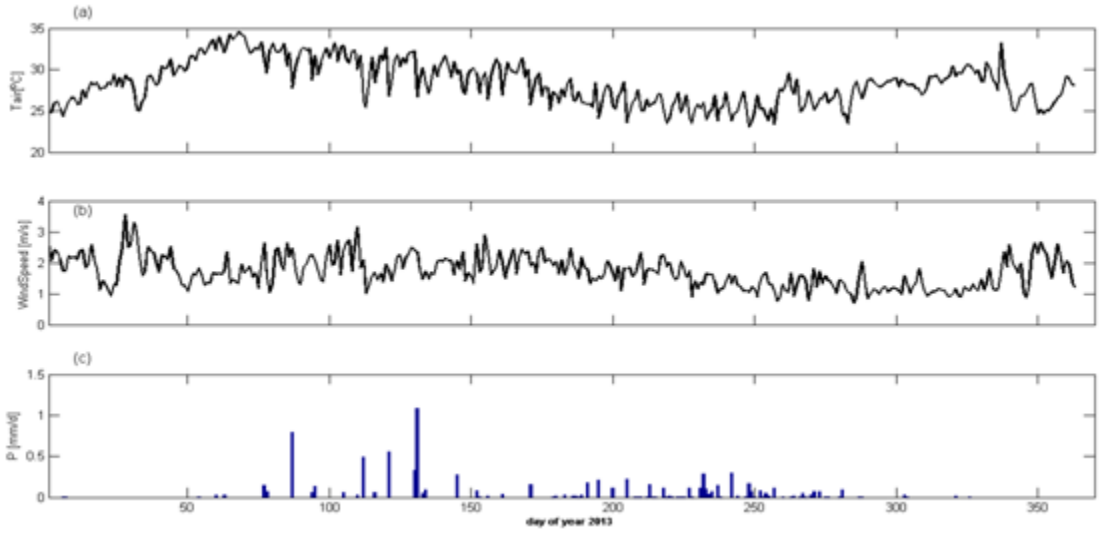

Figure 3a: Daily Averages of Meteorological Parameters, (a) air temperature, (b) wind speed and (c) Precipitation, in the EC station for the year 2013.

All of these meteorological indicators have a distinct seasonal cycle (wet and dry seasons) that is typical of the research area's sudanian savannah climate. Dry-to-wet transition periods and wet-to-dry transition periods separate the wet and dry seasons. The monsoon cycle, which is defined by widely divergent atmospheric and surface conditions, leads to various variation of sensible and latent heat fluxes, that drives these four seasons (wet, dry, dry-to-wet, and wet-to-dry). Lothon et al., 2008 and also in Sultan and Janicot, 2003, demonstrated that the zonal wind and the water vapor mixing ratio (WVMR) may be used to identify the seasons, whereas Mamadou et al., 2014 employed the absolute humidity (qa) determined by the gas analyser to do differentiate the seasons. The dry season was defined as absolute humidity less than 6 gm^{-3}, while the wet season was defined as absolute humidity that are greater than 16 gm^{-3}. The approach employed by Mamadou et al., 2014 was used in this study, although absolute humidity less than 9 gm^{-3} was classified as dry season, and absolute humidity greater than 17 gm^{-3} as rainy season. Between January and February, which is characterized by complete dry season was marked by a steady, low absolute humidity (less than 9 gm^{-3}), a light to moderate breeze (mean 2.4ms-^{1}), and dry air

ISSN: 2455-6939

Volume: 08, Issue: 01 "January-February 2022"

(*qa* greater than 5 gm^{-3}) brought by a dry north-easterly harmattan wind (mean windspeed of 1.9 m^{-2}, mean vapour pressure deficit of 31.5 hPa).

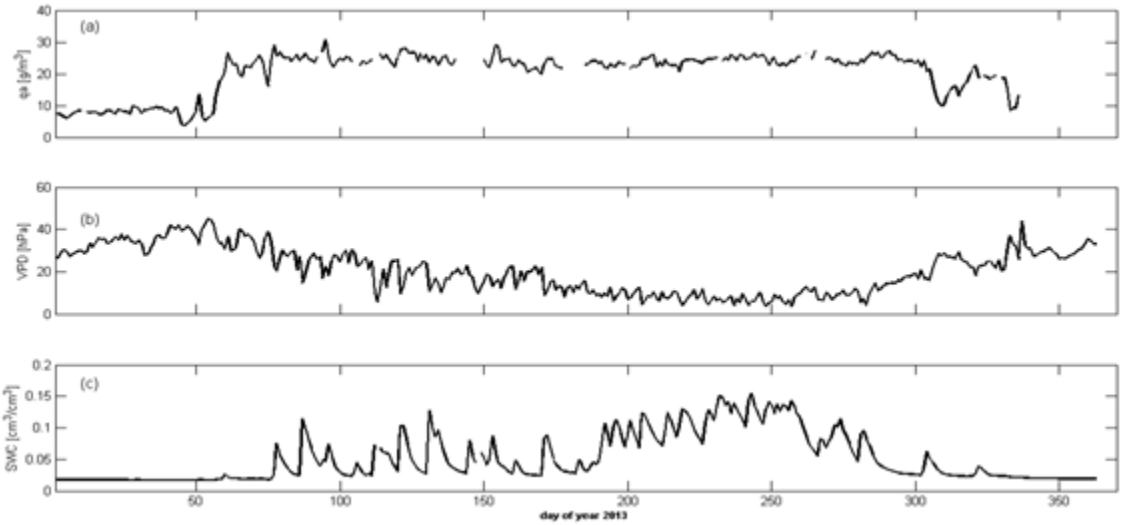

Figure 3b: Daily Averages of Meteorological Parameters, (a) absolute humidity, (b) vapour pressure deficit, and (c) soil water content, in the EC station for the year 2013.

The surface conditions were dry at the time, with no rain, as evidenced by the soil water content SWC, which was found to have a mean of 0.017 cm^3 cm^{-3} at a depth of 3cm. After then, there is a transition phase from the dry to the wet season (February 26th to March 14th). Moist air was advected from the Gulf of Guinea during these monsoonal wind conditions, as evidenced by the significant rise in absolute humidity (mean value of 21 gm^{-3}) at the site. A damp, southerly monsoon flow defined the rainy season (between May and October). The absolute humidity was constant with limited day-to-day change during this season, with a mean of 23.97 gm^{-3}. The SWC was calculated to be 0.07cm^3 cm^{-3} on average. The transition from wet to dry season began at the end of the wet season, when there was no rain (between November 3rd and November 16th). With a mean absolute humidity of 0.026, the soil surface began to dry but was not entirely dry. The mean air temperature $T_{mean(air)}$ was similar to that of the rainy season (28.02°C on average). The air temperature fluctuated during the day. The maximum daily $T_{mean(air)}$ for the site was 34.73°C in March during the dry season, while the lowest daily $T_{mean(air)}$ for the site was 23.27°C in September during the rainy season. The site has an annual mean air temperature of 28.34 °C. The windspeed at the site was generally low, ranging from a daily mean of 0.71 to 3.56 m/s, as seen in figure 4. During the dry season, the wind blew from the north and northeast direction, with a resultant vector of 34 degrees. Dry and dusty air was advected from the Sahelian areas under this harmattan situation. During the rainy season, the wind blew from the

ISSN: 2455-6939

Volume: 08, Issue: 01 "January-February 2022"

south-southwest direction. During this season, the resultant wind vector was 204°. Moist air was advected from the Gulf of Guinea under these monsoonal wind conditions.

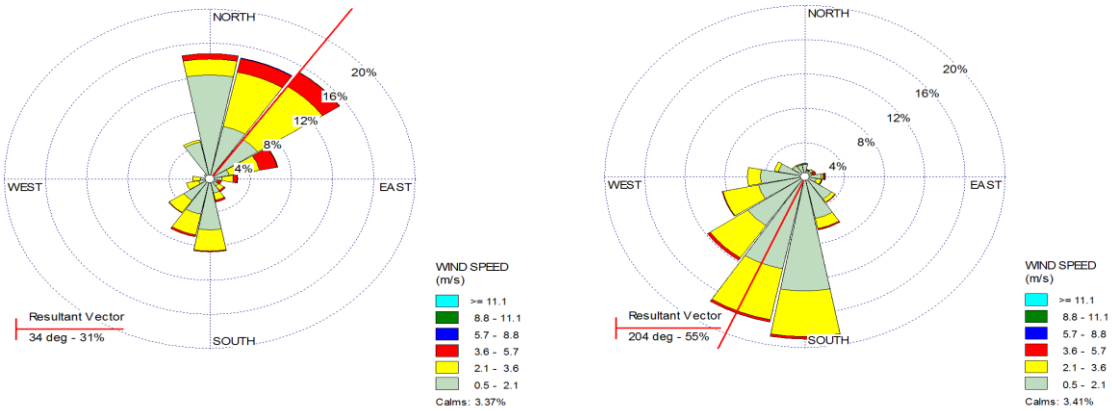

(a) (b)

Figure 4: Wind direction; (a) during the dry season, (b) during the wet season.

The relative humidity RH for the station, as shown in Figure 5, was relatively constant during the dry season, with a mean value of 14 %, and progressively increased to a peak in September, when the monsoon flow was firmly established for the site. The site's daily averaged RH ranged from 7.86 to 93.28 %. The RH reached its lowest point of 7.86 % in February during the dry season, and reached its highest point of 93.28 % in September during the wet season. RH fluctuated in response to changes in precipitation.

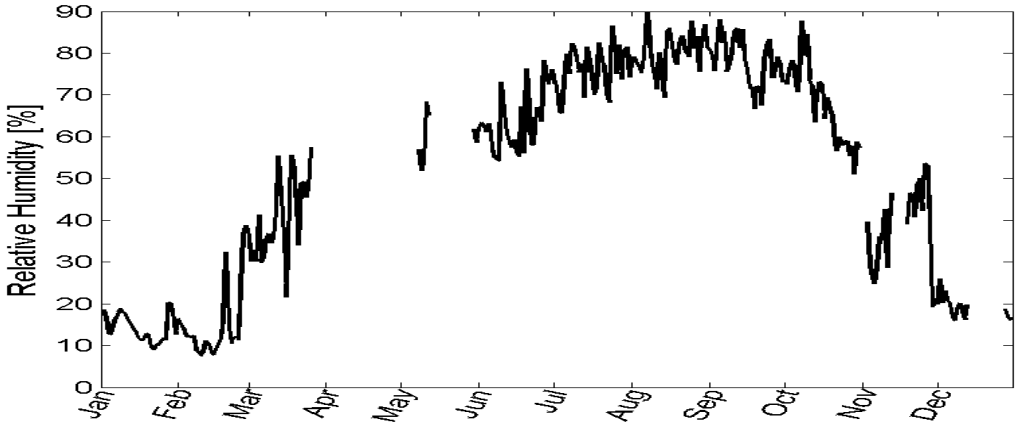

Figure 5: Daily Average of Relative Humidity for the site in the year 2013.

ISSN: 2455-6939

Volume: 08, Issue: 01 "January-February 2022"

3.2 Diurnal variation on monthly average of the Radiation Components.

The monthly mean of the diurnal average of the four radiation components; the incoming longwave radiation (represented by *LW-in*), the outgoing longwave radiation (represented by *LW-out*), the incoming shortwave radiation (represented by *SW-in*) and the out-going shortwave radiation (represented by *SW-out*), are presented in Figure 6 for the site. The values of both *SW-in* and *SW-out* for the diurnal monthly variations remained high during the dry season and began to drop in value from the beginning of the wet season (in the month of May) until reaching a minimum value in the month of August. The diurnal monthly variation of *LW-out* was similar to that of *SW-in* and *SW-out*. On the contrary, the diurnal monthly variation of *LW-in* was completely different, such that, it maintained low values during the dry season and started to increase from the beginning of the wet season to reach a maximum value in August.

In the EC station, the maximum daytime value of *SW-in* and *SW-out* occurred in February at around 14:00 hour reaching 876.60 ± 44.21 Wm^{-2} and 284.85 ± 17.41 Wm^{-2} respectively. The minimum daytime value of *SR-in* and *SR-out* occurred in August at around 14:00 hour, reaching 629.67 ± 240.41 Wm^{-2} and 132.82 ± 50.80Wm^{-2} respectively. The maximum daytime of *LW-out* occurred also in February around 16:00 hour, reaching 76.09 ± 5.85Wm^{-2} and a minimum daytime value in September around 16:00 hour reaching 6.14 ± 5.49 Wm^{-2}. Also, the maximum daytime value of *LW-in* occurred in August at about 16:00 hour, reaching -52.13 ± 21.70 Wm^{-2} while, a minimum daytime value was observed in February at about 16:00 hour, reaching -41.64 ± 18.59 Wm^{-2}. The fluctuation in the incoming radiation during the wet season, especially in the month of August for the site was found to be high. During the wet season, the primarily climate elements that are pre-eminent are water vapour and cloud, and they varies both in time and in space. These elements are majorly responsible for the reflection and attenuation of the incoming solar radiation, thereby causing a reduction in the values of the incoming radiation during this month (Iqbal 1983, Kyle 1991, Jegede 1997). Likewise, the above reason, contribute to the low values of the outgoing longwave, and high values of incoming longwave during the wet season. Whereas, during the dry season, the sky is mostly clear with little or no cloud to attenuate or reflect the incoming solar radiation, as such, the values of the net solar radiation is high, also, the valves of the outgoing longwave radiation is high and the values of the incoming longwave radiation is low.

ISSN: 2455-6939

Volume: 08, Issue: 01 "January-February 2022"

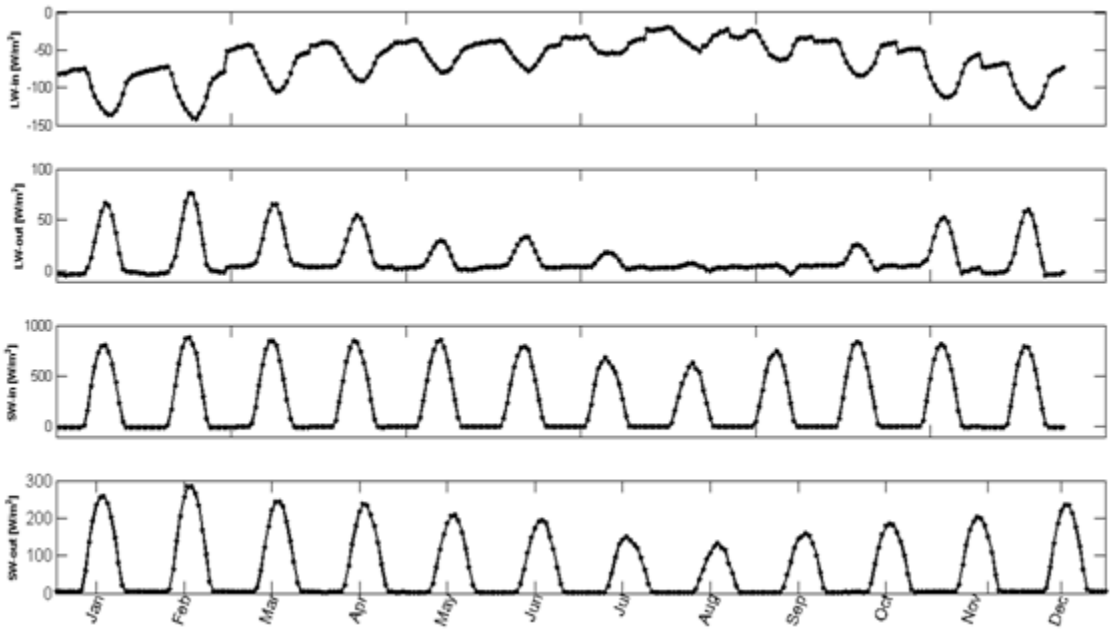

Figure 6: Diurnal monthly averages of the Radiation Components in the EC station.

3.3 Monthly Diurnal Variations of Surface Radiative Fluxes

Radiative fluxes at the surface are the dominant driving force of the surface energy balance. Figure 7 to 8 shows the monthly diurnal variations of the net short wave radiation, represented by *SWnet* (*SWnet = SWin – SWout*), the net long wave radiation represented by *LWnet* (*LWnet = LWin – LWout*) and the net radiation (R_n*= SWnet + LWnet*) for January to December in 2013 at the site. Positive value of the net radiation indicate radiative heating at the surface, while negative values of the net radiation indicate radiative cooling at the surface. The value of net radiation flux was reported to be negative and generally consistent from the early hours of the day (00:00 hour) to around 07:00 hour, with magnitudes varying between -87 and about -12Wm^{-2}, indicating radiative cooling during this period. The net radiation shifts to a positive value after 07:00 hours and steadily increases to a maximum of roughly 539 Wm^{-2} around 1:00 hours. The amplitude of the net radiation declines steadily in the late hours of the afternoon, reaching a minimum value around 18:00 hour as the sun sets. Afterwards, the sign of the net radiation changes to negative with a fairly stable value throughout the evening hours.

ISSN: 2455-6939

Volume: 08, Issue: 01 "January-February 2022"

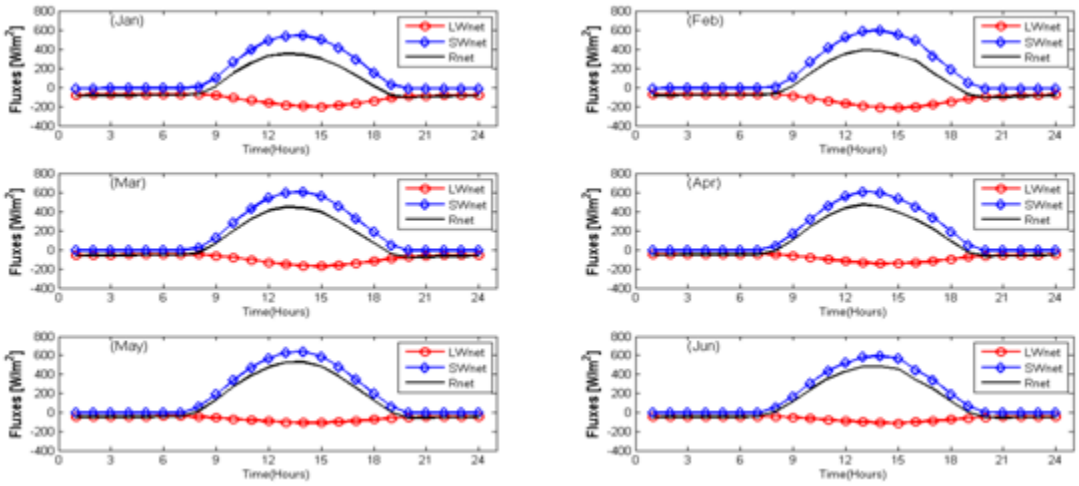

Figure 7: Monthly Diurnal average of Surface Radiative Fluxes from January to June in the EC station.

From January to December, there was a monthly variation in the magnitude of hourly average net radiation, which corresponded to the transition from dry to rainy season. The net radiation value at 14:00 hours in January was determined to be the lowest among the other months of the year. During this month, the harmattan wind (originating in the Sahelian and Saharan regions) transports significant amounts of dust, which makes up air aerosol, which scatters and absorbs solar radiation reaching the earth's surface (Adedokunet al., 1989, Drees et al., 1993). This causes reduction in visibility of the atmosphere, relative humidity and air temperature. The highest daily net radiation value for the months of February and March increased significantly. In addition, from January to March, values of *LWnet* in the night were substantially negative and during the day, the values were high, indicating that surface heating dominates (*LWout* > *LWin*) during the day and the opposite is true at night.

ISSN: 2455-6939

Volume: 08, Issue: 01 "January-February 2022"

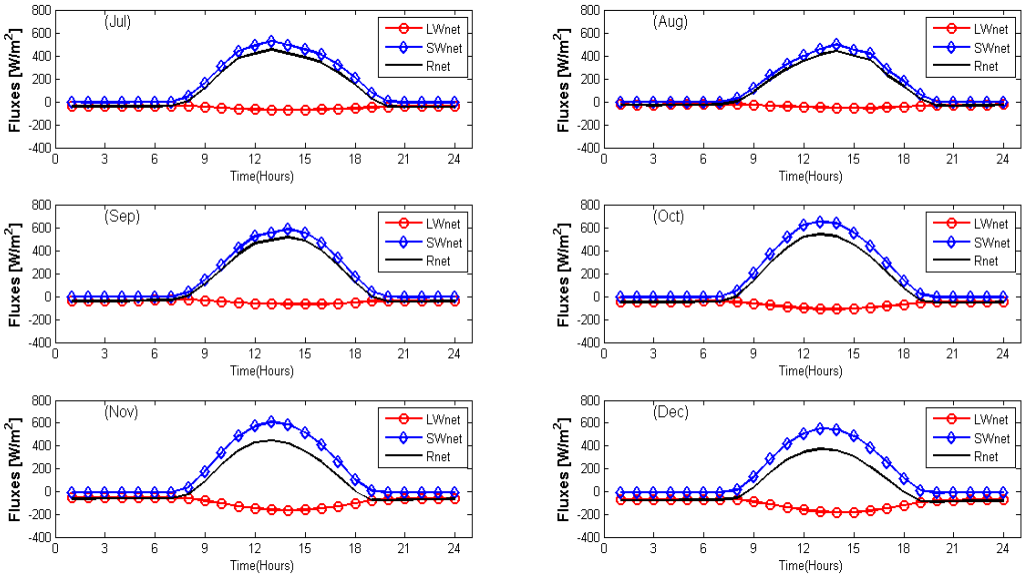

Figure 8: Monthly Diurnal average of Surface Radiative Fluxes from July to December in the EC station.

In April, the surface heating diminishes gradually, with a slight increase in net radiation compared to prior months. The daytime *LWnet* increased throughout the months of May, June, July, and August, when the rainy season had been established at the location, since clouds and water vapour in the atmosphere, re-emit energy. The lowest amounts of net radiation were seen during the peak of the wet season, between July and August. This could be due to frequent cloud cover, resulting in lower net radiation values in the months. During these months, *SWnet* accounts for more than 90% of Rn. From September and December, during the day, net radiation and net shortwave radiation were both higher than in previous months, and incoming shortwave radiation was particularly high in October and November, so surface heating begins to dominate from October onwards. As the wind shifts from the southwest to northeast, the amount of incoming longwave radiation decreases, resulting in an increase in net longwave radiation (just as it affect the month of January).

3.4 Energy Partitioning

Closure of the surface energy budget is a frequent criterion for eddy-covariance flux quality (Wilson et al., 2002, Foken et al., 2004). The quality of the eddy covariance data at the station was assessed using 30 minutes average fluxes of Rn, G, H, and LE from January to December 2013 (number of data points (N) = 12240). The slope and intercept of a straight line regression fit between the turbulent flux (the total of the sensible and latent heat fluxes, H+LE) and the

ISSN: 2455-6939

Volume: 08, Issue: 01 "January-February 2022"

available energy (that is, the net radiation minus soil heat flux, Rn -G) were used to make this determination. For the station, Figure 9 shows the contrast between (H+LE) and (Rn -G). For the station, the slopes of the regression were 0.67, with an intercept of 33 Wm^{-2}. The slope value indicates that the site's energy balance closure is reasonable. Because a lack of closure of the surface energy budget by 10% or more is not uncommon at eddy flux sites, the station's result was judged to be within the range of a typical closure of an EC measurement. Despite the fact that the EC measurements were corrected for measurement errors, the sum of turbulent heat fluxes (H+LE) is typically 10–30% less than Rn – G. (Twine et al., 2000, Richardson et al., 2006). Some studies (Foken and Oncley, 1995, Panin et al., 1996; Wilson et al., 2002, Beyrich et al., 2006; Xu et al., 2017; Mauder et al., 2020) claimed that the reason for the unclosed energy budget were not only related to uncertainties in individual energy component measurements, but also to the influence of different footprints on individual energy components. The soil heat flow was measured at only one place at our site; this point may not be fully typical of the entire site, and the footprints of these energy components (net radiation, sensible heat, latent heat, and soil heat fluxes) are not constant. Large-scale transport of eddies, which cannot be quantified with an eddy covariance technique, has also been blamed for the remaining imbalance in the surface energy budget (Foken 2008). The energy imbalance that was observed was caused by these factors, as well as the inherent inaccuracies that occurred in the individual energy component measurements.

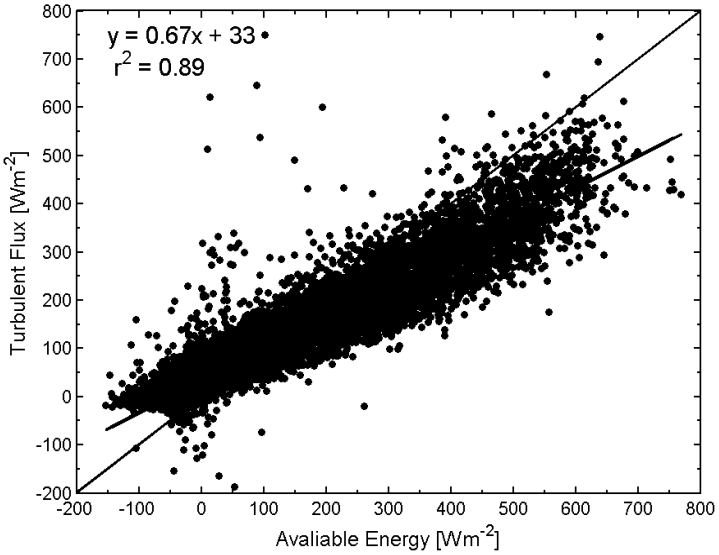

Figure 9: Energy balance closure for 2013 at the station.

ISSN: 2455-6939

Volume: 08, Issue: 01 "January-February 2022"

3.5 Seasonal variation of sensible heat flux, latent heat flux and Net Radiation

Figures 10 to 12 demonstrate the seasonal change in daily net radiation, sensible heat flux, and latent heat flux for the site. During the dry season, the latent heat flux for the location is rather stable when averaged over 24 hours for each day (Figure 12), with a comparatively low value, less than $10Wm^{-2}$. At the end of March, there was a slight increase. Daily variations in the latent heat flux occurred throughout the wet season, with peak daily values occurring between April and October. The availability of energy in the form of net radiation Rn and the partitioning of this energy (Rn) into latent heat, sensible heat, and ground heat are the primary constraints on the magnitude of the sensible and latent heat flux. The annual daily average of net radiation for the station, which is in a grassland area, is low. The availability of soil moisture and grass vegetation in the site are the primary cause of differences in net radiation during the dry season. In the peak of the rainy season at the site, two main occurrences result in enhanced surface net radiation. The first factor is plant growth, which is triggered by rainfall. In view of the fact that, an increase in leaf area reduces surface albedo and hence, reduces long wave radiation losses (Samain et al., 2008). The availability of soil moisture is the second factor that leads to higher net radiation during the rainy season (Lobell and Asner, 2002), because the availability of water on the surface, favours latent heat flux over sensible heat flux; it increases surface cooling and reduces long wave radiation losses, thus increasing net radiation. Because the factors driving the increase in Rn also change the surface flux partitioning toward increased latent heat flux than sensible heat flux, the seasonal increase in net radiation coincides with a decrease in sensible heat flux.

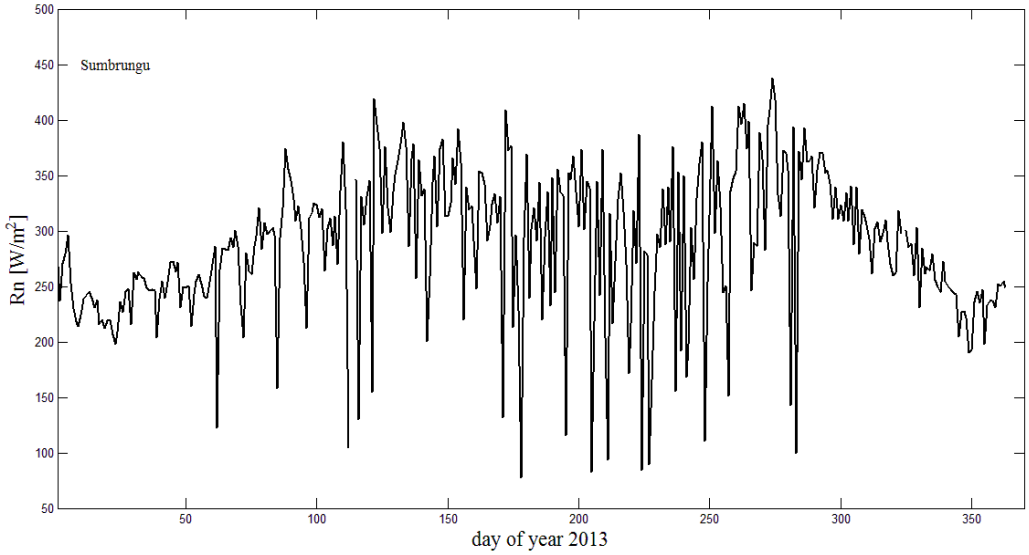

Figure 10: Seasonal Variation of Net Radiation (Rn) in the EC station

ISSN: 2455-6939

Volume: 08, Issue: 01 "January-February 2022"

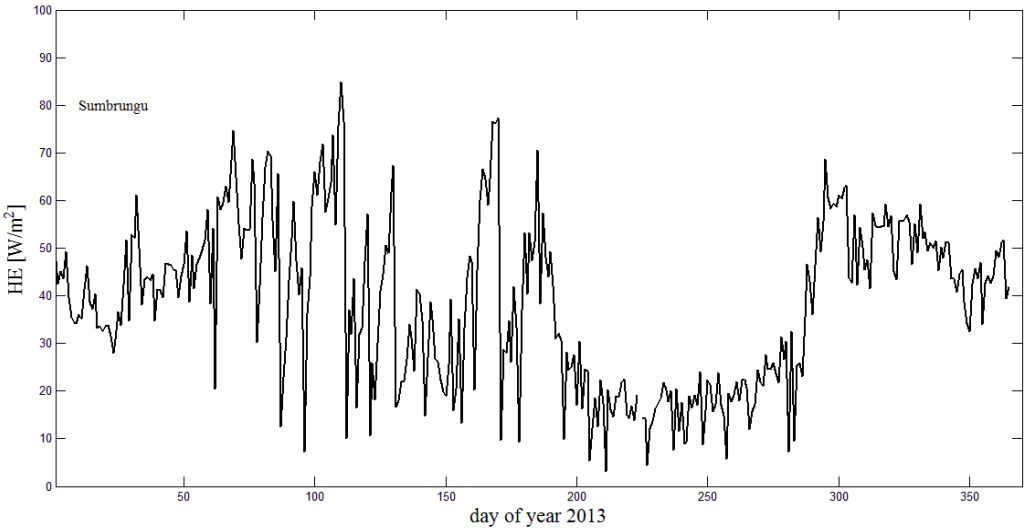

Figure 11: Seasonal Variation of Sensible heat flux in the EC station

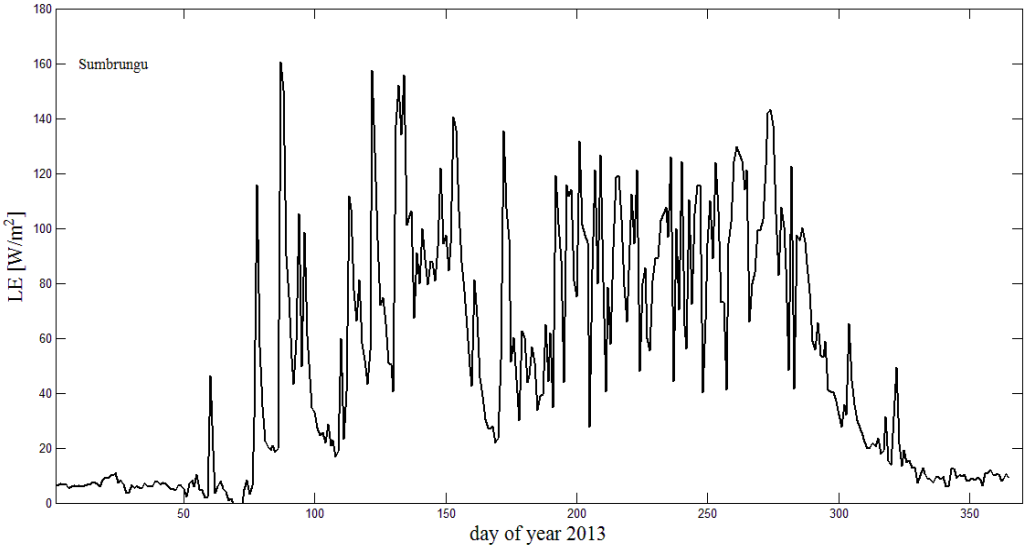

Figure 12: Seasonal Variation of Latent heat flux (LE) in the EC station.

3.6 Seasonal Variation of Surface Characteristics

3.6.1 Surface Albedo

Figure 13 depicts the annual daily average of the site's surface albedo. The surface albedo is strongly related to the vegetation seasonal cycle, which is driven by precipitation. The value of

ISSN: 2455-6939

Volume: 08, Issue: 01 "January-February 2022"

the surface albedo was found to be high throughout the dry season, peaking at 0.38 at the end of the dry season, and started to decrease at the beginning of the rainy season that commenced in March until the end of November, afterward, the value of the surface albedo began to increase again until the end of December. The station's daily average albedo ranged from 0.20 to 0.38. The high albedo values (with mean values of 0.31 ± 0.033) were recorded during the dry season, when most of the leaves were already dry, withered, and shriveled, and the sensible heat flux was more pronounced. During the rainy season, lower values of surface albedo (mean values of 0.36 ± 0.027) were found. Vegetation growth and changes in Soil Water Content modify the absorbance and reflectance characteristics of the soil, resulting in decreased mean surface albedo during the rainy season. The amount of incident solar radiation absorbed by the soil system increases as the Soil Water Content rises. Moisture in the soil absorbs incident radiation, lowering the surface albedo.

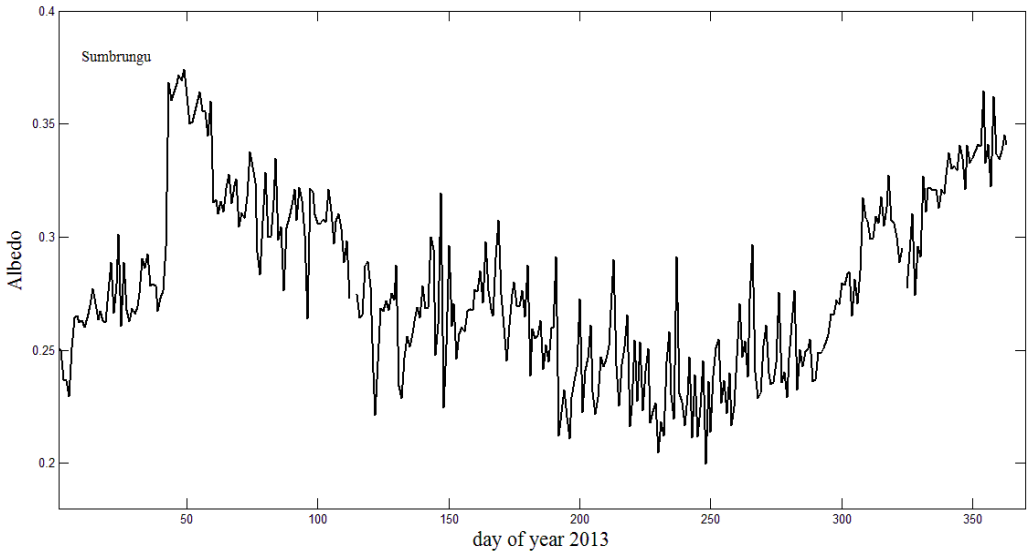

Figure 13: Seasonal Variation of surface albedo in the EC station.

3.6.2 Evaporative Fraction

Seasonal variations in EF are a reflection of the local climate, particularly rainfall and soil moisture (Farah, 2004). It is a particularly effective indicator of soil or vegetation moisture levels at a site because high amounts of energy partitioned into latent heat flux indicates a healthy, transpiring vegetation and low values indicates moisture stress. Figure 14 depicts the seasonal variation of EF. Each point reflects the average value from 9:00 a.m. to 17:00 p.m. Low EF values were found in the site during the dry season, with an average value of 0.19 ± 0.13. In the

ISSN: 2455-6939

Volume: 08, Issue: 01 "January-February 2022"

site, higher EF values were reported during the rainy season, with an average value of 0.66 ± 0.19, indicating a response to increased soil moisture over the station.

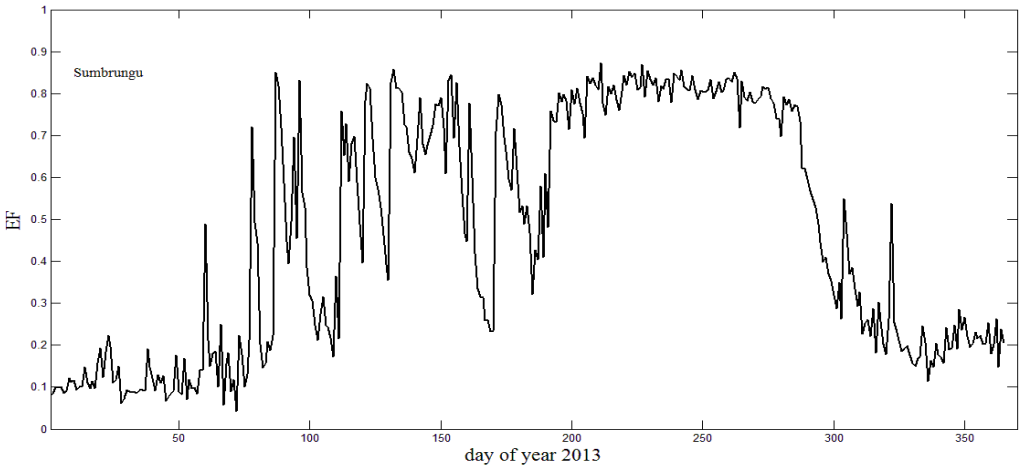

Figure 14: Seasonal Variation of Evaporative fraction (EF) in the EC station.

3.6.3 Bowen Ratio

Figure 15 shows a plot of the Bowen ratio Bo, which is the ratio of sensible heat flux to latent heat flux from a surface to air. With respect to the evaporative fraction, the graph exhibited the opposite behaviour. When the soil surface was wet during the wet season, the Bowen's ratio values was small. These low values were caused by the simultaneous transfer of a little amount of sensible heat and a significant amount of latent heat. When the soil surface is dry (during the dry season), the Bowen's ratio is high due to a considerable transport of sensible heat and a small exchange of latent heat.

ISSN: 2455-6939

Volume: 08, Issue: 01 "January-February 2022"

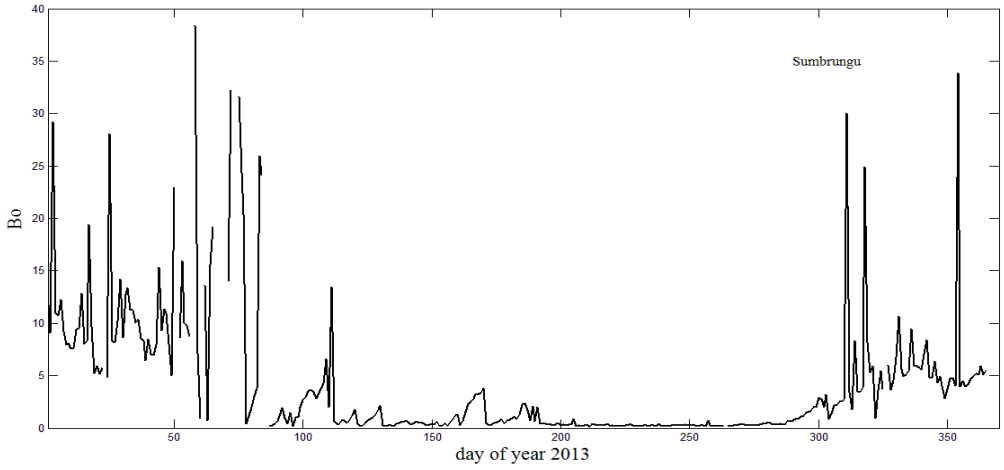

Figure 15: Seasonal Variation of Bowen ratio (B_O) in the EC station.

4. CONCLUSION

The available energy, which is predominantly driven by incoming solar radiation, drove the seasonal variation in the latent and sensible heat fluxes at the EC station (installed at Sumbrungu Agunsi). The incoming and outgoing shortwave radiation, as well as the incoming and outgoing longwave radiation, changes differently, causing a seasonal variation in net radiation. During the wet season, latent heat was stronger than sensible heat, whereas during the dry season, sensible heat was stronger. During the wet season, the latent heat flux was more pronounced, whereas during the dry season, the sensible heat flux was more pronounced. The slope of the regression was 0.67, with an intercept of 33 Wm^{-2} and r^2 of 0.67, when surface energy partitioning was investigated at the site. The following are thought to be the causes of the energy imbalance problem: the soil heat flux was measured at only one point, which may not be a full representation of the entire site; the footprints of net radiation, sensible heat, latent heat, and soil heat fluxes are inconsistent; and the unavoidable uncertainties in the individual energy component measurements. The soil moisture content was found to be low during the dry season but increased during the rainy season, causing most of the available energy to be converted to latent heat. Also, as soil moisture content and vegetation cover increase, surface albedo drops; as soil moisture content and vegetation cover decrease, surface albedo increases, at the site. Due to the low amount of sensible heat flux transported to the air, the average seasonal change in Bowen ratio was small during the wet season. During the dry season, however, due to a considerable amount of latent heat flux transported to the air, the average seasonal variation of the Bowen ratio was large. Similarly, due to minor rainfall occurrences, the evaporative fraction was found to be high during the wet season and low during the dry season.

ISSN: 2455-6939

Volume: 08, Issue: 01 "January-February 2022"

ACKNOWLEDGEMENT

We acknowledge the financial support from BMBF for the installation and maintenance of the EC and automatic weather station at the study area.

REFERENCES

[1] Adedokun, J.A., Emofurieta, W.O. and Adedeji, O.A. (1989). Physical, mineralogical and chemical properties of Harmattan dust at Ile-Ife, Nigeria. *Theoretical and Applied Climatology* 40, 161–169.

[2] Beljaars, A. C. M., and A. A. M. Holtslag (1991). Flux parameterization over land surfaces for atmospheric models, J. Appl. Meteorol., 30, 327–341.

[3] Beyrich, F., Leps, J., Mauder, M., Bange, J., Foken, T., Huneke, S., Lohs, H., Andreas Lu Di, Wouter M. L. Meijninger, DmitriiMironov, Ulrich Weisensee and Peter Zittel (2006). Area-averaged surface fluxes over the litfass Region based on eddy-covariance measurements. *Boundary-Layer Meteorology* 121:33–65.

[4] Brutsaert, W., and Sugita, M. (1992). Application of self-preservation in the diurnal evolution of the surface energy budget to determine daily evaporation. *Journal of Geophysical Research* 97. 377-382.

[5] Charney, J. G. (1975). Dynamics of deserts and drought in the Sahel, Q. J. Roy. Meteorol. Soc., 101, 193–202, 1975.

[6] Callo-Concha, D., Gaiser, T. and Ewert, F. (2012). Farming and cropping systems in the West African Sudanian Savanna. WASCAL research area: Northern Ghana, Southwest Burkina Faso and Northern Benin. ZEF Working Paper 100. Bonn. 48 pp.

[7] De Vries, D.A. (1963). *Thermal Properties of Soils. In Physics of Plant Environment*. Edited by VanWijk WR, North-Holland Publishing Company Amsterdam, pp. 210 – 235.

[8] Dickinson, R. E., A. Hendersin-Sellers, C. Rosenzweig, and P. J. Sellers (1991). Evapotranspiration models with canopy resistance for use in climate models, a review, Agric. For. Meteorol., 54, 373–388.

[9] Dixon, J., Gulliver, A. and Gibbon, D. (2001). Farming system and poverty: Improving Farmers' Livelihoods in a Changing World. Rome and Washington DC: FAO and the World Bank (2002), pp. 412.

[10] Drees, L.R., Manu, A. and Wilding, L.P. (1993). Characteristics of aeolian dusts in Niger, West Africa.Geoderma 59, 213–233.

[11] Farah, H.O., Bastiaanssen, W.G.M., and Feddes, R.A. (2004). Evaluation of the temporal variability of the evaporative fraction in a tropical watershed, *International Journal of Applied Earth Observation and Geoinformation* 5: 129-140.

[12] Foken, T. (2008). The energy balance closure problem: An overview. Ecological Applications, 18:1351 - 1367.

[13] Fuller D. O. and Ottke C. (2002). Land Cover, Rainfall and Land-Surface Albedo In West Africa. *Climatic Change* 54: 181–204

[14] Foken, T., Göckede, M., Mauder, M., Mahrt, L., Amiro, B. and Munger, W. (2004). Post-field data quality control. Handbook of Micrometeorology. A guide for surface flux measurement and analysis. Kluwer Acad. Publ., Dordrecht, the Netherlands, 181–208.

[15] Foken, T., and Oncley, S. P. (1995). Results of the workshop Instrumental and methodical problems of land surface flux measurements. B. Am. Meteorol. Soc., 76, 1191–1193

[16] Iqbal, M. (1983). An Introduction to Solar Radiation. Iqbal, M. Editorial. Academic Press, Toronto, Canada.

[17] Jegede, O. O. (1997). Diurnal variations of net radiation at a tropical station – Osu, Nigeria. *Theor. Appl. Climatol*. 58, 161-168.

[18] Jegede, O.O., Mauder ,M., Okogbue, E.C., Foken, T., Balogun, E.E., Adedokun,J.A., Oladiran, E.O., Omotosho J.A., Balogun, A.A., Oladosu, O.R., Sunmonu, L.A., Ayoola, M.A., Aregbesola, T.O., Ogolo, E.O., Nymphas, E.F.,Adeniyi, M.O.,Olatona, G.I., Ladipo, K.O., Ohamobi, S.I., Gbobaniyi ,E.O. and Akinlade, G.O. (2004). The Nigerian Micro Meteorological Experiment (NIMEX-l): AN OVERVIEW. *Ife Journal of Science* vol. 6, no.2. pp 191- 202.

[19] Kyle, T. G. (1991). Atmospheric Transmission, Emision and Scattering. Oxford: Pergamon Press, 288 pp.

[20] Liebethal, C., Huwe, B. and Foken, T. (2005). Sensitivity analysis for two ground heat flux. calculation approaches. *Agric For Meteorol*. 132.253–262. (doi. 10.1016/j.agrformet.2005.08.001)

[21] Lobell, D.B. and Asner G.P. (2002). Moisture effects on Soil Reflectance. Soil Sci. Soc. Am. J. 66:722-727.

[22] Lothon, M., Saïd, F., Lohou, F., and Campistron, B. (2008). Observation of the Diurnal Cycle in the Low Troposphere of West Africa, Mon. Weather Rev., 136, 3477–3500.

[23] Mamadou, O., Cohard, J.M., Galle, S., Awanou, C.N., Diedhiou, A., Kounouhewa, B. and Peugeot, C. (2014). Energy fluxes and surface characteristics over a cultivated area in Benin: *Daily and seasonal dynamics. Hydrol. Earth Syst. Sci.,* 18, 893–914. (doi:10.5194/hess-18-893-2014).

[24] Massman, W. J. and Lee, X. (2002). Eddy Covariance Flux Corrections and Uncertainties in Long Term Studies of Carbon and Energy Exchange. *Agric. For. Meteorol*. 113, 121–144.

ISSN: 2455-6939

Volume: 08, Issue: 01 "January-February 2022"

[25] Mauder, M., Jegede, O. O., Okogbue, E. C., Wimmer, F., and Foken, T. (2007). Surface energy balance measurements at a tropical site in West Africa during the transition from dry to wet season, Theor. Appl. Climatol., 89, 171–183.

[26] Mauder, M. and Foken, T. (2011). Documentation and Instruction Manual of the Eddy - Covariance Software Package TK3. Abteilung Mikro meteorologie, Universität Bayreuth, Arbeitsergebnisse 46.

[27] Mauder M., Foken T. and Cuxart J. (2020). Surface-Energy-Balance Closure over Land: A Review. Boundary-Layer Meteorol 177, 395–426. doi.org/10.1007/s10546-020-00529-6

[28] Nicholson, S. E., Tucker, C. J., and Ba, M. B. (1998). Desertification, Drought, and Surface Vegetation: An Example from the West African Sahel. *Bull. Amer. Meteorol. Soc.* 79, 815–829.

[29] Oluwadare Ayoola O., Okogbue Emmanuel C., Kunstmann Harald, Akinluyi Frank, Arnault Joel, Tayari Salisu, Hingerl Luitpold and Bliefernicht Jan (2018). Comparison of SEBAL Estimated Heat Fluxes and Evapotranspiration using Field and Remote Sensing Data in the Sudanian Savanna in West Africa. International Journal of Agriculture and Environmental Research, Volume 4, Issue 2, pp. 352 – 374.

[30] Panin, G. N., Tetzlaff, G., Raabe, A., Sch¨onfeld, H. J. and Nasonov, A. E. (1996). Inhomogeneity of the land surface and the parameterization of surface fluxes – a discussion. Wiss Mitt Inst Meteorol Univ Leipzig und Inst Tropospharenforschung Leipzig 4: 204–215.

[31] Richardson, A.D., Hollinger, D.Y., Burba, G.G., Davis, K.J., Flanagan, L.B., Katul, G.G., Munger, J.W., Ricciuto, D.M., Stoy, P.C., Suyker, A.E., Verma, S.B. and Wofsy. S.C. (2006). A multi-site analysis of random error in tower-based measurements of carbon and energy fluxes. *Agricultural and Forest Meteorology* 136:1-18.

[32] Samain O., Kergoat L., Hiernaux P., Guichard F., Mougin E., Timouk F., Lavenu F. (2008). Analysis of the *in situ* and MODIS albedo variability at multiple time-scales in the Sahel. *Journal of Geophysical Research* **113**: D14119. DOI: 10.1029/2007JD009174.

[33] Schotanus, P., Nieuwstadt, F.T.M., and De Bruin, H.A.R.D. (1983). Temperature measurement with a sonic anemometer and its application to heat and moisture fluxes. *Boundary Layer Meteorology*, 26. pp 81–93.

[34] Sultan, B., and Janicot, S. (2003). The West African monsoon dynamics, Part II: The "Preonset" and the "Onset" of the summer monsoon. J Clim.16:3407–27.

[35] Taylor, C. M. and Lebel, T. (1998) Observational evidence of persistent convective-scale rainfall patterns, Mon. Weather Rev., 126, 1597–1607.

[36] Taylor, C. M., de Jeu, R. A. M., Guichard, F., Harris, P. P., and Dorigo, W. A. (2012). Afternoon rain more likely over drier soils, Nature, 489, 423–426.

[37] Toda, M., K. Nishida, N. Ohte, M. Tani, and K. Musiake (2002). Observations of energy fluxes and evapotranspiration over terrestrial complex land covers in the tropical monsoon environment, J. Meteorol. Soc. Jpn., 80(3), 465– 484.

[38] Timouk, F., Kergoat, L., Mougin, E., Lloyd, C. R., Ceschia, E., Cohard, J.M., de Rosnay, P., Hiernaux, P.,Demarez, V. and Taylor, C. M. (2009). Response of Surface Energy Balance to Water Regime and Vegetation Development in a Sahelian Landscape, *Journal of Hydrology*, Vol. 375, No. 1-2, pp. 178-189. (doi:10.1016/j.jhydrol.2009.04.022).

[39] Twine, T.E., Kustas, W.P., Norman, J.M., Cook, D. R., Houser, P.R., Meyers, T.P., Prueger, J.H, Starks, P.J. and Wesely, M.L. (2000). Correcting eddy-covariance flux underestimates over a grassland. *Agric. For. Meteorol*. 103, 279 – 300.

[40] United Nations, Department of Economic and Social Affairs, Population Division (2019). *World Population Prospects 2019: Highlights* (ST/ESA/SER.A/423).

[41] Verhoef, A., Allen, S.J., De Bruin, H.A.R., Jacobs, C.M.J. and Heusinkveld, B.G. (1996). Fluxes of carbon dioxide and water vapour from a Sahelian savanna. *Agricultural and Forest Meteorology* 80, 231–248.

[42] Vickers, D. and Mahrt, L. (1997). Quality control and flux sampling problems for tower and aircraft data. *J Atmos Ocean Technol* 14. 512-526.

[43] Webb, E.K., Pearman, G.I., Leuning, R. (1980). Correction of the flux measurement for density effects due to heat and water vapour transfer. *Q J R Meteorol Soc* 106.85-100.

[44] Wilczak, J.M., Oncley, S.P. and Stage, S.A. (2001). Sonic anemometer tilt correction algorithms. *Bound Layer Meteorol* 99. 127-150.

[45] Wilson, K., Goldstein, A., Falge, E., Aubinet, M., Baldocchi, D., Berbigier, P., Bernhofer, C., Ceulemans, R., Dolman, H., Field, C., Grelle, A., Ibrom, A., Law, B.E., Kowalski, A., Meyers, T., Moncrieff, J., Monson, R., Oechel, W., Tenhunen, J., Valentini, R. and Verma, S. (2002) Energy balance closure at FLUXNET sites. *Agricultural and Forest Meteorology* 113. 223–243. Xu Z., Ma Y., Liu S., Shi W. and Wang J. (2017). Assessment of the energy balance closure under advective conditions and its impact using remote sensing data. J Appl Meteorol Climatol 56:127–140. https://doi.org/10.1175/JAMC-D-16-0096.1

[46] Xue, Y., Juang H. H.-M., Li W., Prince S., DeFries R., Jiao Y., and Vasic R. (2004). Role of land surface processes in monsoon development: East Asia and West Africa, J. Geophys. Res., 109, D03105, doi:10.1029/2003JD003556.

